JOURNAL OF APPLIED ELECTROCHEMISTRY 17 (1987) 1234–1245

Electrochemical phenomena in aqueous electrowinning of lead

MAGDY GIRCIS*, EDWARD GHALI

Department of Mining and Metallurgy, Laval University, Quebec, Canada G1K 7P4

Received 9 April 1987

Attempts have been made to electrowin smooth and compact lead deposits from a medium containing glycine and hydrochloric acid, since this solution was recommended for its capacity to dissolve lead salts. Numerous factors such as electrolyte composition, current density, temperature, stirring and working electrodes were considered in the search for better quality deposits. Linear and cyclic sweep voltammetry, and potentiostatic and galvanostatic perturbations were employed in order to examine the processes at the cathode and to interpret the influence of some organic compounds added to the bath. Surface analyses of the lead deposit were performed by X-ray diffraction, scanning electron microscopy and Auger electron spectroscopy.

1. Introduction

The prospect of producing lead metal from its sulphide ores, mainly galena, through a direct electrowinning process from aqueous chloride solutions has recently attracted scientific and industrial interest. The incentive for the new trend is great since the traditional pyrometallurgical and fused salt processes require higher energy and tighter regulations to control the lead smelter environment. The process of electrodissolution of galena resulted in a precipitation of some residual products such as $PbCl_2$ [1].

MacKinnon [2] reviewed the present state-of-the-art of the electrowinning of lead from aqueous chloride electrolytes. He concluded that deposits obtained by different processes [3–6] are characteristically non-compact and powdery, even at low current densities. In previous trials [7, 8], electrodeposition of lead from aqueous solutions containing ammonium acetate and acetic acid was investigated. The studies revealed that ammonium acetate has a strong capacity in dissolving $PbCl_2$, and compact deposits could be obtained for certain electrolyte compositions containing some additive agents.

Glycine also showed a certain activity in dissolving lead salts, especially $PbCl_2$ [9], and its addition to an acidic aqueous solution containing chloride ions was found to be effective in preventing anodic passivation caused by $PbCl_2$ during electrodissolution of galena [10]. It therefore seems pertinent to investigate the electrowinning process on the cathode and to seek better operating conditions for the electrowinning of compact and smooth lead deposits from an aqueous medium containing glycine and hydrochloric acid. According to the literature this system has not yet been studied. The addition of organic compounds such as phenol, ethyl alcohol and gelatine was tried in order to obtain lead deposits which are more compact and smooth. The studies on the deposition process were carried out using different electrochemical perturbation techniques such as linear and cyclic sweep voltammetry, chronoamperometry and chronopotentiometry. The results were compared to those obtained from a fluoborate solution which has important application in the lead industry. Surface analyses and the morphology of lead deposits were examined by X-ray diffraction analysis, scanning electron microscopy (SEM) and Auger electron spectroscopy (AES).

* *Present address*: Department of Chemistry, Carleton University, Ottawa, Canada K1S 5B6.

0021–891X/87 $03.00 + .12

2. Experimental details

Polycrystalline Teflon-embedded substrates of 99.99% purity, i.e. lead, copper, silver, aluminium and spectrographic graphite, were used as working electrodes with an apparent surface area of 5 cm^2 for all electrodes except silver (0.129 cm^2). Graphite and saturated calomel electrodes served as auxiliary and reference probes respectively. The electrodes were rinsed and mechanically polished before being transferred to the electrolytic cell. The experiments were conducted using BDH 'Analar' grade reagents of $PbCl_2$, glycine (CH_2NH_2COOH) and HCl, and were made up with bidistilled water. Oxygen was purged from the cell by bubbling nitrogen through the electrolyte for 45 min before each experiment. Studies in the fluoborate bath were carried out according to the method described by Blum *et al.* [11]. The electrolyte was prepared by slowly adding boric acid (74 $g\,l^{-1}$) to 50% HF (160 $g\,l^{-1}$). The solution was then allowed to cool and was stirred while basic $2PbCO_3 \cdot Pb(OH_2)$ (129 $g\,l^{-1}$) was added.

A Tacussel potentiostat (type PRT 20-2X) equipped with plug-ins (type TP PRT) as a waveform generator was used to monitor the desired potential and to vary the sweep rate. Linear potential sweeps and potentiostatic and galvanostatic transients were recorded on a Honeywell 540 X–YY recorder. The experimental set-up and cell design are described elsewhere [7]. The surface analyses were performed with a varian Auger microprobe, model Escalab-500 VG Scientific Ltd, to analyse the top layer of the lead deposits at normal incidence. The base pressure of the system was 10^{-8} Torr. The operating conditions are described later (see Results and Discussion). The morphology of lead crystal lattice were examined using an SEM model JEOL-2553.

3. Results and discussion

3.1. *Choice of bath and morphology of deposit*

3.1.1. Glycine medium. After a series of preliminary investigations an optimum concentration of 2.1 M glycine was chosen to dissolve 0.11 M $PbCl_2$. The quantity of lead chloride was fixed during the experiments, since some preliminary investigations showed that deposits obtained from electrolytes containing high concentrations of $PbCl_2$ (> 0.2 M) were of crystalline nature and showed a tendency to form trees, while lower concentrations (< 0.05 M) resulted in poor deposits. When high concentrations of glycine (> 2.5 M) were tried, the pH of the electrolyte approached the range of neutrality, pH $\approx$ 6, and recrystallization of glycine was observed due to the effect of the dipolar structure ($CH_2\overset{+}{N}H_3CO_2^-$). However, it was found that the deposition process in the latter case required imposition of a high current density (> 30 mA cm^{-2}). It is possible that the species formed in the electrolyte are mainly Pb(glycine)$_2$, Pb(glycine)$^{2+}$ and/or Pb(glycine)$_2^{2+}$ and are hardly dissociated. The evidence for the formation of lead–glycine species may be presented as follows.

(i) If $PbCl_2$ were the only electroactive species in the solution (i.e. no lead–glycine formation) the deposition potential would have been observed at values more anodic to those found in our system. Harrison *et al.* [12] reported that lead chloride is reduced at -0.450 V.

(ii) A literature survey confirmed the presence of such a complex formation between Pb^{2+} ions and glycine. In this regard, Milazzo and Caroli [13] quoted from Monk [14] that the probable complex species are Pb(glycine)$^{2+}$ and Pb(glycine)$_2^{2+}$ with reduction potentials of -0.288 and -0.388 V vs NHE respectively. Monk also reported that at low pH values, PbR_2 formation is very small (where R is the glycine radical).

Because of the poor quality of lead deposits, i.e. their dendritic nature on all the cathodes used, and the low current efficiency (65%), HCl was added to increase the conductivity of the supporting electrolyte.

3.1.2. Glycine–hydrochloric acid medium. Since the addition of 5 M HCl to a solution of 2.1 M glycine was found efficient for the electrodissolution of galena [10], an attempt was made to use these concentrations to recover lead from 0.11 M $PbCl_2$ with a view to developing a new method of electrowinning lead directly from galena in aqueous solutions. The lead deposit obtained from this bath was adherent but of a dendritic

nature on lead, copper and silver substrates at 45° C under both stirred and unstirred conditions at a current density of 20 mA cm^{-2}. Under the same conditions the deposit was of non-compact crystals on aluminium and carbon cathodes. The bath deteriorated after 15 min of electrolysis, a yellow colour being developed in the clear solution. A tendency to form dendritic lead, especially at the edges of the cathodes was observed after 20 min of electrolysis. In addition to the presence of lead–glycine species as discussed earlier, species of $[CH_2NH_3CO_2H]Cl^-$ [15], $[CH_2NH_3CO_2C_2H_5]Cl^-$ [16] and lead chloride complexes such as $PbCl_2$, $PbCl^+$, $PbCl_3^-$ and $PbCl_4^{2-}$ [17] are also likely to form. The development of the yellow colour during the electrolysis could be interpreted as a result of direct anodic oxidation of chloride ions. In an attempt to solve the problem of bath deterioration we attempted to neutralize the excess HCl or to stabilize the pH by adding bases such as Na_2CO_3, $NaHCO_3$, NaOH and triethanol amine, but the results were discouraging since high quantities were required to buffer the acid.

3.1.3. Additive agents. In a previous study [7], a good quality lead deposit was successfully obtained by adding a combination of phenol, ethyl alcohol and gelatine to a bath composed of $PbCl_2$ and CH_3COONH_4. Similar results were obtained when these additives were added to the glycine–HCl bath, where the deposits became more compact and smooth on the lead and copper substrates. A tendency to form dendrites was observed on the silver cathode. The results were not encouraging enough on the carbon and aluminium substrates, where no improvement in the quality of the deposit was shown. It was also found that the presence of these additives helped solve the problem of bath deterioration. The optimum operating conditions of the bath were: 30 g l^{-1} $PbCl_2$, 160 g l^{-1} glycine, 5 M HCl, 20 ml l^{-1} phenol, 40 ml l^{-1} ethyl alcohol and 0.3 g l^{-1} gelatin, 45° C, 20 mA cm^{-2} at moderate stirring conditions. The current efficiency was in the 90–95% range for the electrodes selected, i.e. lead, copper and silver substrates. X-ray diffraction patterns for the deposits obtained from the glycine–HCl media in the absence and in the presence of the organic additives showed a pure lead deposit, while in the glycine medium alone the deposit was contaminated by $PbCl_2$. The scanning electron micrographs (Fig. 1) show the effect of the organic additives on the morphology of the lead deposit. The crystals become more dense and of fine structure.

3.1.4. Factors affecting deposit quality. Different studies were carried out to show the effect of different parameters on the deposit obtained from the bath containing glycine–HCl in the presence of organic additives. Dendritic lead was formed when a current density in a range of 25–50 mA cm^{-2} was imposed, especially at high temperature (> 50° C) and in unstirred solutions. In the range 10–20 mA cm^{-2}, a smooth and compact deposit was formed at 45° C under moderate magnetic stirring. At higher current density (> 50 mA cm^{-2}) a powdery lead deposit was obtained. Moderate stirring (magnetic) was found necessary to obtain a good quality lead deposit. The effect of substrate was also important. A smooth and compact deposit was obtained when silver, copper and lead substrates were used at 45° C in a moderately stirred solution at current densities of 10–20 mA cm^{-2}. When aluminium and carbon electrodes were used the tendency to form dendrites and large non-compact crystals was observed at all temperatures used and in both stirred and unstirred solutions. The deposition process on the surface of aluminium and carbon was obviously slow and hydrogen evolution was vigorous on the surface of the aluminium electrode, possible due to retardation of lead deposition.

3.2. *Electrochemical investigation*

Further insight on the mechanism of the deposition process and on the role of the organic additives was achieved by employing different electrochemical techniques. Only the results obtained when silver, lead and copper electrodes were used are discussed in this communication, since on both the aluminium and carbon substrates the deposit was not adherent and was spongy. We will refer to the media under study, i.e. glycine–HCl, glycine–HCl in the presence of organic additives, and fluoborate as baths 1, 2 and 3 respectively.

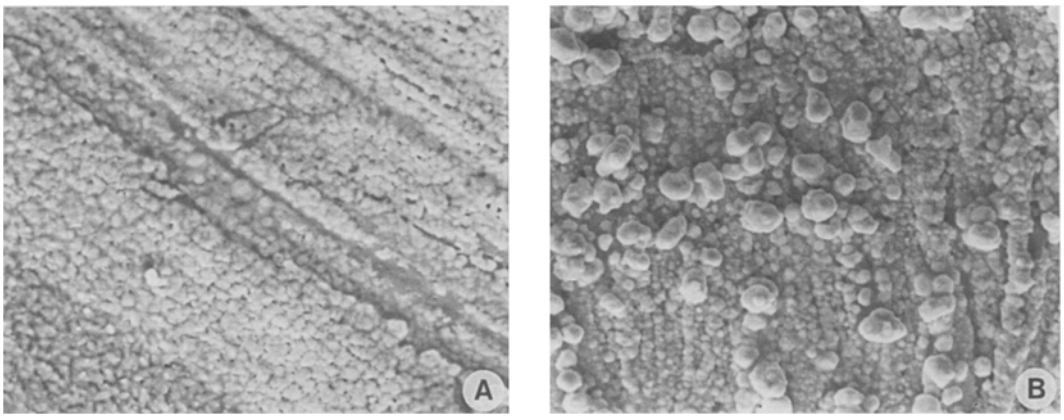

Fig. 1. SEM pictures of lead deposits on silver electrode at 45° C and 20 mA cm^{-2} after 20 min of electrolysis from stirred solutions of (A) glycine–HCl and (B) glycine–HCl in the presence of the organic additives.

3.2.1. Linear sweep voltammetry. In all the media studied, the cyclic voltammograms recorded for both copper and silver electrodes were characterized mainly by two main ranges of potential over which distinguishable cathodic processes occur, i.e. UPD and bulk deposition regions, respectively, followed by an anodic peak upon scan reversal. The absence of an anodic peak when the lead electrode was used is evident (Fig. 2) due mainly to the irreversible nature of the reaction mechanism. The deposition potential did not differ from bath 1 to bath 2 (−0.61 V), thus indicating that the reduced species are the same and are most likely Pb(glycine)$^{2+}$ and/or Pb(glycine)$_2^{2+}$, as mentioned earlier. Only a slight difference in the case of the silver electrode was observed for bath 1 (−0.61 V) and bath 2 (−0.63 V) and this was confirmed by repeating the experiment many times. The deposition potential in the case of bath 3 was the same for the three substrates (−0.38 V), due probably to reduction of $Pb(BF_4)_2$ to Pb metal and $2BF_4^-$. The latter might form fluoboric acid and some of its hydroxy derivatives, e.g. $HBF_3(OH)$ and $HBF_2(OH)_2$.

3.2.1.1. UPD region. It was difficult to determine the exact deposition potential in the UPD region, but it had approximate values of −0.47 V for baths 1 and 2 and of −0.2 V for bath 3, as shown in Fig. 3.

The total cathodic charge in the UPD region was dependent on the medium and on the substrate. The data in Table 1 demonstrate that the presence of the organic additives resulted in lowering the cathodic charges calculated for

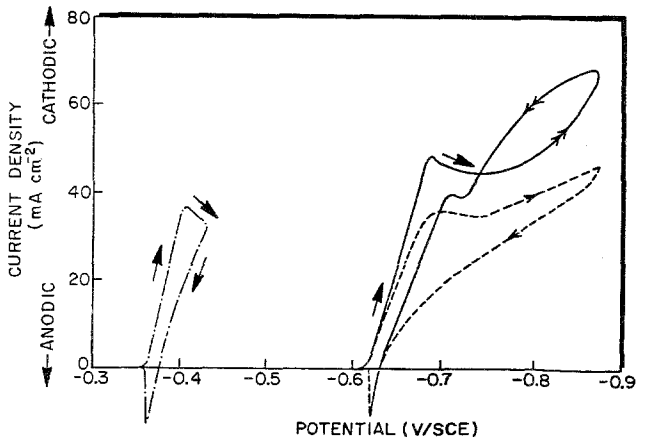

Fig. 2. Cyclic voltammogram of lead deposition on lead electrode from bath 1 (——), bath 2 (– – –) and bath 3 (–·–·–) at 45° C under unstirred conditions (50 mV s^{-1}).

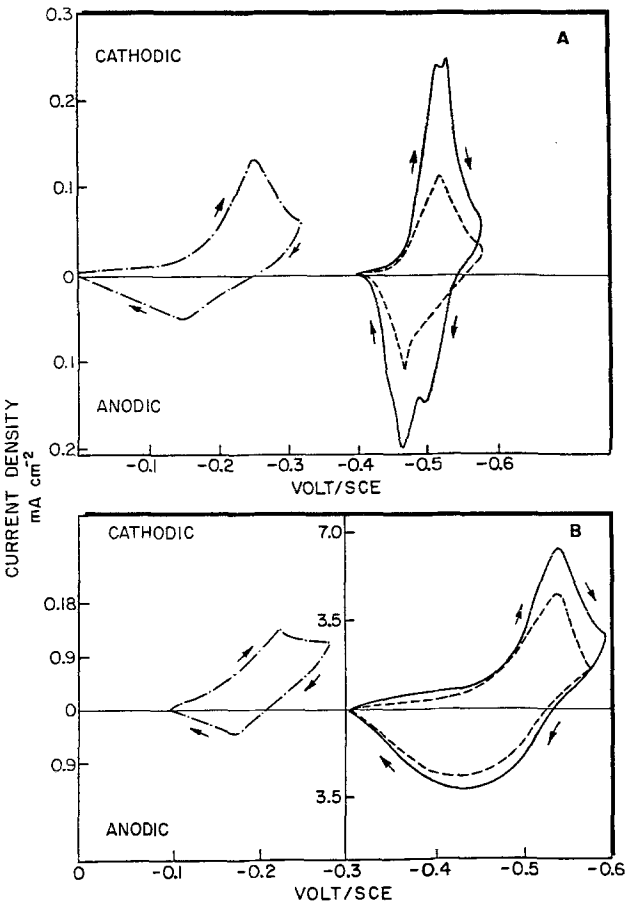

Fig. 3. Cyclic voltammograms of lead deposition on (A) copper and (B) silver substrates in the underpotential range from bath 1 (——), bath 2 (– – –) and bath 3 (–·–·–) at 45° C under unstirred conditions ($v = 50\,mV\,s^{-1}$).

bath 2, in comparison to bath 1. Considering that the theoretical value for a close-packed lead monolayer is $302\,\mu C\,cm^{-2}$, we may emphasize that different factors play an important role in the UPD region, Cl^-/substrate effect or Pb/substrate effect and/or both. In the literature, Kolb [18] quoted from Schmidt and Wüthrich [19] and Stucki [20] that the Cl ion is not adsorbed as an ion but obviously forms a compound with silver and gold electrodes. Also, Westall *et al.* [21] reported that copper has a tendency to form a stable complex with Cl ions of type ($CuCl^+$). In view of the above statements we can assume that this effect of the Cl ion on the substrate in our study might enhance the formation of monolayers in the case of silver electrodes, while lowering its formation rate in the case of copper electrodes. The high values for the total charge passed before the onset of the bulk deposition for the silver electrode can also be attributed to the commencement of lead deposition on the top of the close-packed monolayer. From the above observation, the lower values of the UPD cathodic charges in bath 2 compared to bath 1 can be attributed to the direct effect of the organic additives in hindering, to a certain extent, the integration of the Cl ions on the substrate surface, thus decreasing any kind of effect that might be exerted by these ions.

Table 1. Calculated charges in the UPD region

Electrode	*Charge, Q ($\mu C\,cm^{-2}$)*		
	Bath 1	*Bath 2*	*Bath 3*
Copper	131	93	207
Silver	7811	5620	237

The theoretical approach to investigate in more detail the effect of various parameters on the behaviour in the UPD region is beyond the

scope of this paper, but further studies are currently in progress.

3.2.1.2. Bulk deposition region. The dependence of the cathodic peak current (i_p) on the square root of potential sweep rate ($v^{1/2}$) was observed for the silver electrode in the absence and in the presence of the additives (Fig. 4) and this suggests that the reaction is under diffusion control according to the equation [22]:

$$I_p = 3.67 \times 10^5 n^{3/2} A D^{1/2} C_0 v^{1/2}$$

where I_p is the peak current ($A\,cm^{-2}$), D is the diffusion coefficient ($cm^2\,s^{-1}$), v is the scan rate ($V\,s^{-1/2}$), n is the number of electrons, and C_0 is the concentration of the electroactive species ($mole\,cm^{-3}$).

Linearity was also achieved for the copper electrode but the curves did not intersect the origin. This implies that lead deposition in this case is controlled by electrocrystallization [23].

In the case of the fluoborate bath, the voltammogram showed no diffusion peak around the deposition potential. Instead, an inductive current loop was observed; this made it difficult to calculate I_p.

Sweeping the scan to a more cathodic potential limit for the three media resulted in a current loop at -0.8 V for bath 1 (Fig. 2) and at ≈ 0.93 V for baths 2 and 3 (not shown in the figure). The formation of this loop is probably due to the rapid growth of the surface in the form of dendrites and the reaction is then characterized by spherical diffusion rather than linear diffusion [24]. This observation leads to a general conclusion that dendritic lead formation is retarded in the presence of addition agents.

The effect of successive sweeps on the voltammograms was similar for both copper and silver electrodes but dependent on the potential region. Quasi-steady-state profiles in the UPD region were achieved for the three media after the first five cycles, indicating a complete adsorption–desorption process. In the potential region (between -0.2 and -0.7 V), the voltammograms exhibited a continuous increase in cathodic peak current (in the deposition region -0.6 to -0.7 V) for bath 1, while steady current–voltage profiles were recorded for baths 2 and 3 after certain successive cycles. This phenomenon could be attributed to an inefficient dissolution process for bath 1 during the anodic sweep and this might have resulted in an increase in the cathode surface area every cycle, thus causing an increase of the cathodic current. For baths 2 and 3 a complete dissolution–deposition process could provide an explanation for the achievement of steady-state profiles. It is worth mentioning that the cycling effect in the potential region -0.2 to -1.0 V was similar for all the substrates and independent of the medium, and resulted mainly in a continuous increase in the deposition current due to a steady roughening of the substrate which may accelerate the nucleation centres, thus promoting dendritic growth. From the above observations we can conclude that the presence of addition agents has the effect of decreasing the possibility of the formation of surface defects (steps, kinks, etc.) which is favoured in media that contain surface-active anions such as Cl ions.

3.2.2. Potentiodynamic studies. In unstirred solutions of baths 1 and 2, the potentiodynamic curves for the three electrodes were characterized by a peak which has the morphology of a diffusion-controlled process around the deposition potential, followed by an increase in the cathodic current (Fig. 5). Under stirred conditions this peak was less well observed. In bath 3 it was hard to observe this peak under either condition. The curves demonstrate clearly that bath 2 is characterized mainly by low current density and high overpotential in comparison to bath 1. This may be the reason for improving the quality of lead deposit to a more dense and compact form. Tafel slope values were calculated for baths 1 and 2 under stirred conditions, where the effect of diffusion is minimized. The values were slightly high for bath 2 and this may be as a result of the additional overpotential created in the solution in the presence of the additives. The values of Tafel slopes as indicated on the η–log (i) curves (Fig. 6) for baths 1 and 2 demonstrate that unipositive lead ions, Pb^+, are formed during cathodic deposition. Similar results were interpreted for zinc deposition by Jung and Jorné [25] who confirmed that cathodic deposition from a chloride medium was first order and postulated that the cathodic mechanism consists of two consecutive one-electron

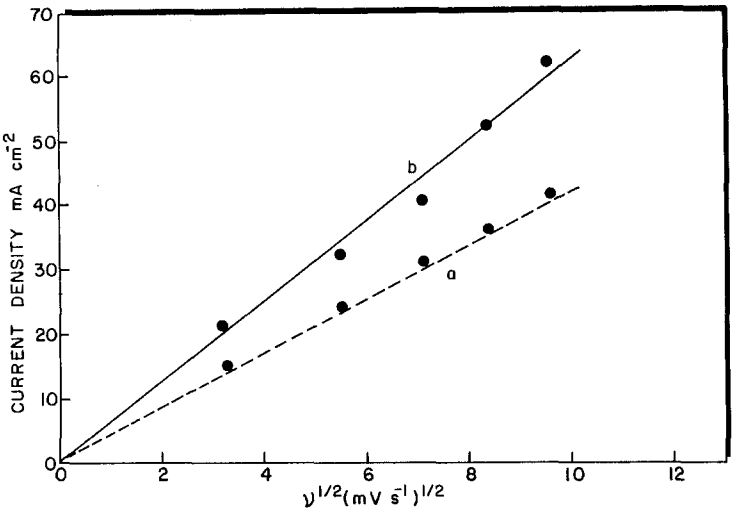

Fig. 4. Dependence of the peak current, i_p, on the scan rate ($\nu^{1/2}$) during deposition of lead on the silver electrode in the bulk deposition region in (a) presence and (b) absence of organic additives at 45° C under unstirred conditions.

transfer steps where the first step is rate determining.

3.2.3. Transient studies. Potentiostatic i–t curves were constructed by imposing different potentials covering different stages of the bulk deposition process. The starting potential was always slightly anodic to the reversible potential of the Pb/Pb^{2+} redox couple as observed from the cyclic voltammetry studies (−0.6 V). Fig. 7

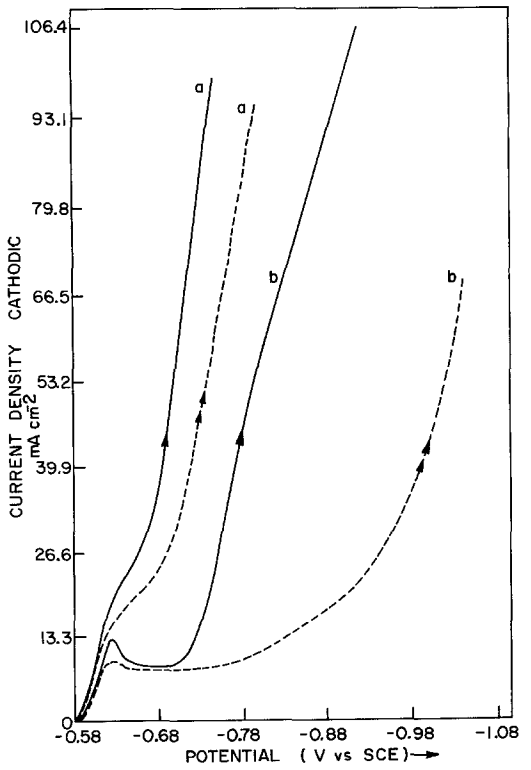

Fig. 5. Potentiodynamic curves for lead deposition from unstirred solutions of bath 1 (——) and bath 2 (– – –) at 45° C (ν = 10 mV s^{-1}) in (a) stirred and (b) unstirred solutions.

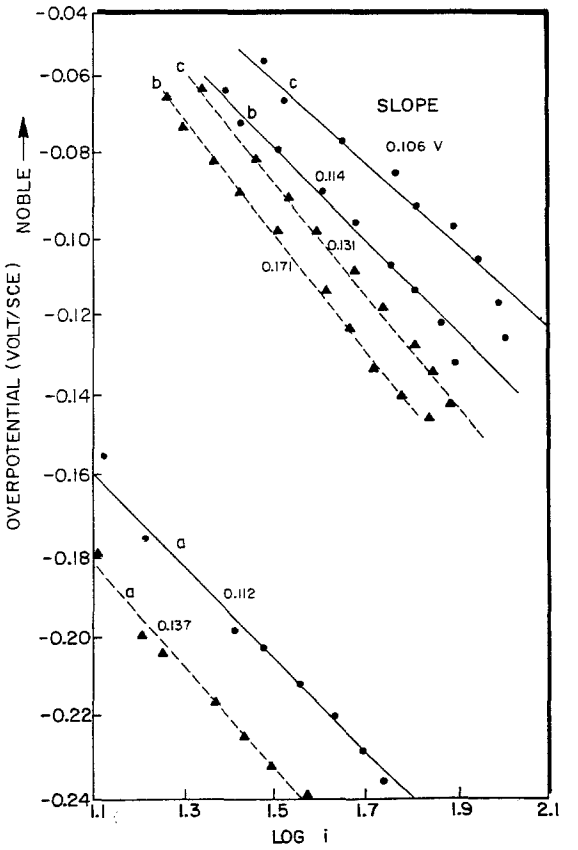

Fig. 6. Calculated Tafel slopes (V) from stirred solutions of bath 1 (——) and bath 2 (– – –) at 45° C. Substrates: (a) silver, (b) lead, (c) copper.

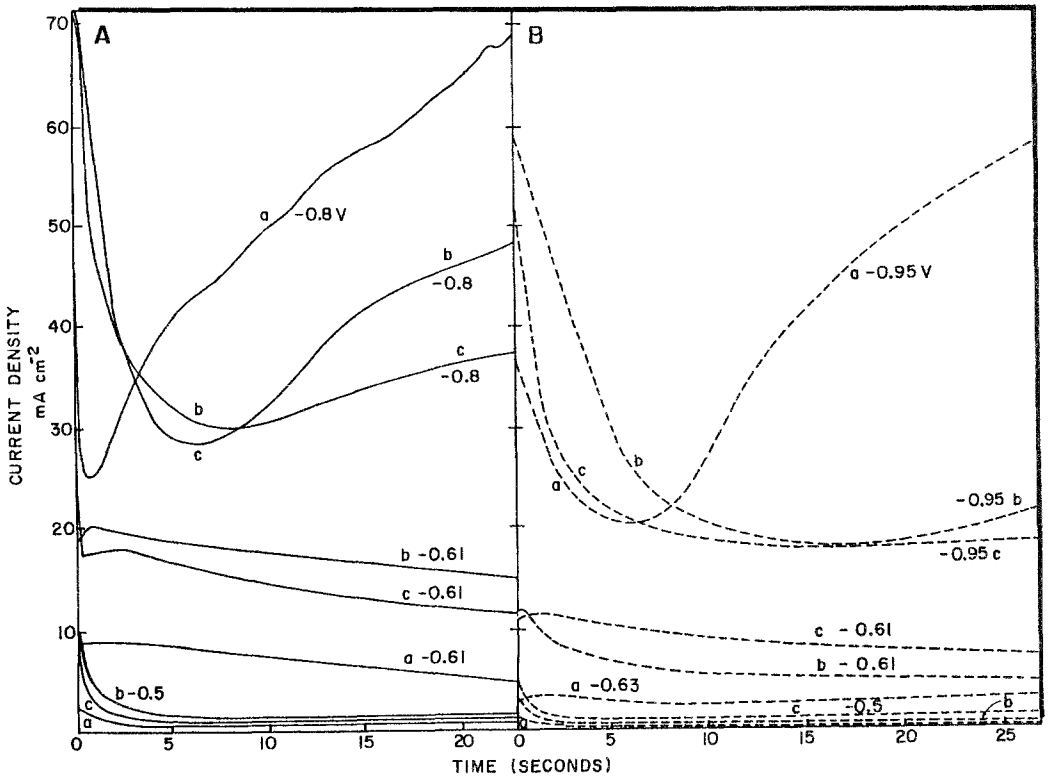

Fig. 7. Potentiostatic current–time transients for lead deposition from unstirred solutions of bath 1 (——) and bath 2 (- - -) at 45° C at different cathodic potentials. Substrates: (a) silver, (b) lead, (c) copper.

shows growth transients for the various stationary electrodes in baths 1 and 2. In all cases, the transients exhibited a current peak at potentials corresponding to the deposition voltages (range -0.61 to -0.63 V) due mainly to the start of lead nuclei formation. As imposed potential increased, the width of this peak (maximum) decreased and i_{max} and t_{max} shifted to shorter times due to rapid growth of the nuclei. When the system was pulsed to high negative potentials, i.e. -0.8 V, where dendritic lead is expected to form, a rapidly falling transient was

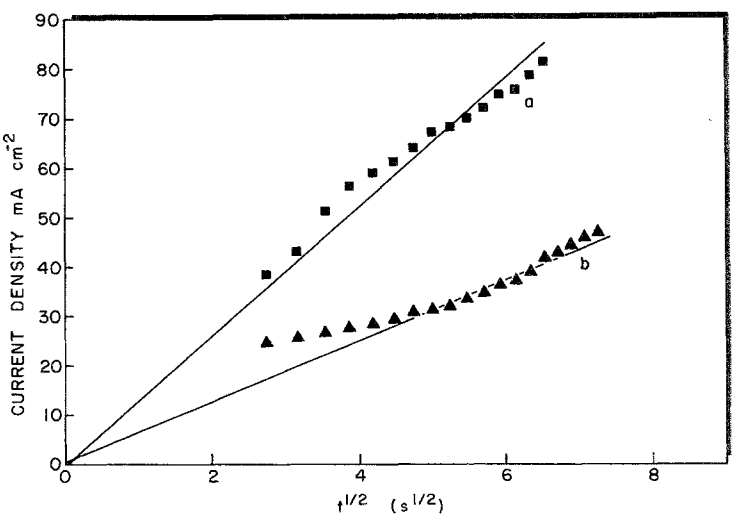

Fig. 8. The i_p–$t^{1/2}$ plot of lead growth on the lead electrode in (a) absence and (b) presence of addition agents at 45° C from unstirred solutions.

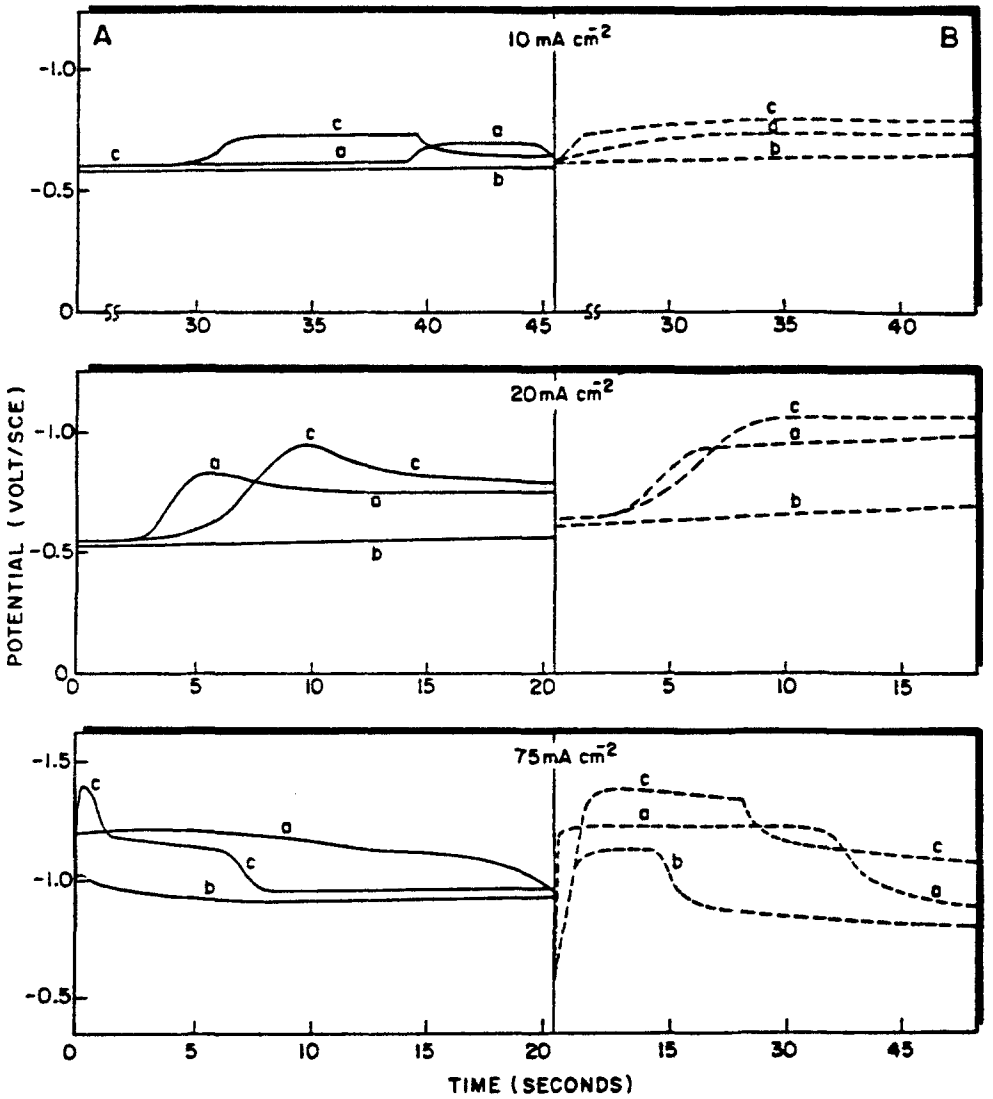

Fig. 9. Galvanostatic potential–time transients for lead deposition from unstirred solutions of bath 1 (——) and bath 2 (– – –) at 45° C at different imposed current densities. Substrates: (a) silver, (b) lead, (c) copper.

observed, followed by a gradual increase in current with time, as expected for multilayer nuclei growth. The three substrates showed the same behaviour.

An analysis of the rising portions of the transients revealed that cathodic currents are linear in $t^{1/2}$ as given by the equation [26]:

$$i = \frac{ZFN_0\pi(2DC_0)^{3/2}M^{1/2}t^{1/2}}{\varrho^{1/2}}$$

where Z is the number of electrons, F is the Faraday constant, N_0 is the total number of the nucleation sites, D is the diffusion coefficient, C_0 is the concentration of the electroactive species, M is the molecular weight, ϱ is the density, and t is the time. This indicates that the reaction is proceeding via an instantaneous three-dimensional nucleation, followed by hemispherical diffusion-controlled growth of the nuclei. This phenomenon was independent of medium and substrates. Fig. 8 shows the i–$t^{1/2}$ plot for the silver electrode in both media, i.e. in the absence and in the presence of organic additives. A similar phenomenon was observed for bath 3, but only at potentials higher than -0.95 V.

Similar to the behaviour in the polarization

curves, the current density was lower in bath 2 than bath 1, due probably to the passivation phenomenon caused by the organic additives. The characteristic features of the $i-t$ curves did not change much upon application of stirring conditions to both baths, but the current density was higher than that obtained in unstirred solutions. Also, the rising transient was at times observed to be shorter than that obtained in unstirred solution, thus confirming that the reaction is not controlled as much by diffusion when a stirring is applied.

The potentiostatic transients suggest that the lead growth process is independent of the medium and this leads to a general conclusion that the role of the additives is confined to the effect of forming a barrier layer near the cathode. This decreases any kind of anion adsorption on the surface (mainly Cl), thus diminishing its deleterious effect in creating atom defects at the cathode surface which promote dendritic growth. Such effects enhance formation of new crystal nuclei and, thus, a finer surface structure [27].

The passive layer formed by the organic additives may also result in the presence of high overpotentials. This fact is presented in the galvanostatic $V-t$ curves. The potential was higher in bath 2 than in bath 1 for the same current density. Imposing a high current density, i.e. 75 mA cm^{-2} (Fig. 9), resulted in the presence of a high overpotential which remained steady with time, followed by a drop in potential probably due to H_2 evolution. The effect of stirring led to the elimination of the polarization peak and a steady overpotential was observed as a function of time. A similar steady relationship between potential and time was observed for bath 3 under unstirred and stirred conditions.

3.3. *Purity of deposit obtained from baths 1 and 2*

Better understanding of impurity behaviour and the role of organic additives was achieved by analysing the deposit using Auger electron spectroscopy. Specimens to be analysed were selected through SEM observations at an electron gun voltage of 10 keV and a current density of 40 mA cm^{-2}. For $N(E)$ spectrum, the step size was eV per channel and for dNE/dE spectra, the numerical data handling were 21 point smooth + numerical differentiation. The Auger spectra for both cases, i.e. in the absence and in the presence of the organic additives, showed some impurities with the deposit, such as Cl, N and O. The initial spectra before any sputtering with assignment of each peak are shown in Fig. 10. The spectra were also characterized by a large peak in the 250–300 eV region, due probably to an overlapping of lead and carbon since both emit signals in this region (lead at 245, 263 eV and carbon at 263 eV) [28].

In order to obtain in-depth information, i.e. to examine the distribution of each element as a function of depth from the original surface, sputter etching using argon ion (5 keV, 10^{-8} Torr) was conducted. The time required to sputter through the deposit was 15 min. Typical Auger spectra of the composition profiles of lead deposits electrowon from baths 1 and 2 are shown in Fig. 10. The spectra reveal that the intensities of the peaks corresponding to the impurities decreased with the etching process, while that of lead increased. The peaks corresponding to nitrogen were of much lower intensity than the other elements and disappeared completely after 2 min of sputtering. A slight effect of the sputtering process on lead deposit was observed in the case of the silver electrode, even after 4 h. The initial rise in the lead signal was remarkable after 25 min of sputtering. This could be attributed to the sputter removal of the adsorbed layers of the impurities. The intensity level was noticeably higher in bath 2. The peaks corresponding to the other elements behaved differently to those of lead. The height of the zero Auger peaks decreased with sputter time and disappeared after 20 min in bath 2, while traces of this peak were still observed for bath 1 even after 1 h. The same behaviour was observed for the peak intensity of Cl, but the spectra revealed traces of Cl in both baths after 1 h (for lead and copper electrodes) and 4 h (for silver electrode), although the intensity was much lower in bath 2. The strong influence of aluminium ions on the substrates, as shown qualitatively from the AES studies, was in the order of Ag $\gg$ Cu $>$ Pb. We can state then that the effect of Cl is strongly dependent on the substrate.

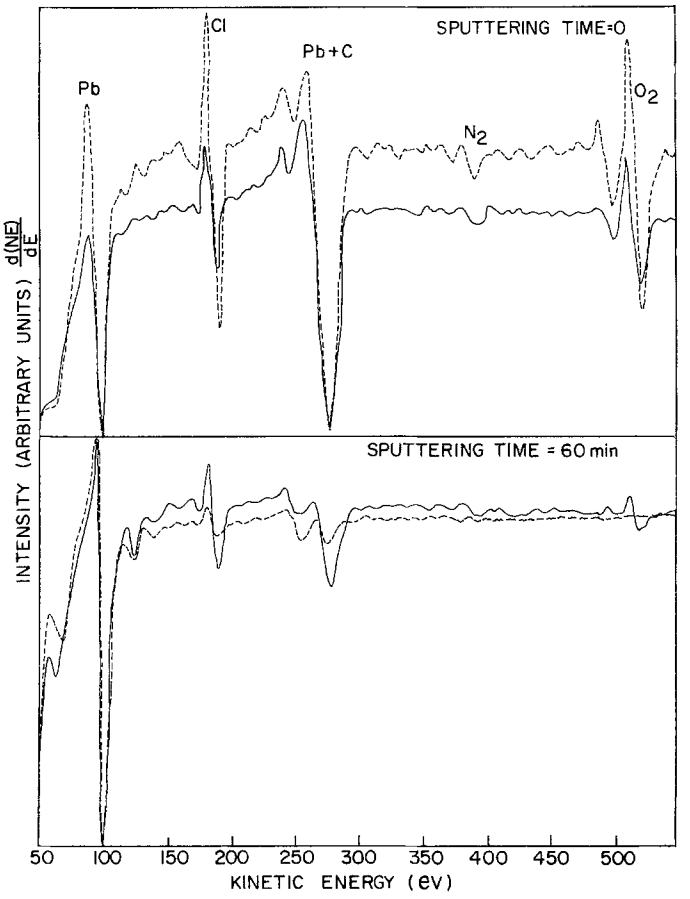

Fig. 10. AES spectra of depth profile of lead on a lead substrate from stirred solutions of bath 1 (——) and bath 2 (– – –) at 45° C and 20 mA cm^{-2}.

In the 250–300 eV region, the height of the peak decreased and levelled off after 20 min of sputtering in bath 2, while in bath 1 the intensity was still high even at a sputtering time of 1 h. This phenomenon could lead to the interpretation that the broad peak in the 250–300 eV region corresponds to both carbon and lead and that carbon is eliminated after 20 min of sputtering in bath 2, while traces of carbon are still observed in bath 1.

In view of these observations, it can be assumed that the organic additives in bath 2 form a passive layer near the cathode which hinders, to a certain degree, the adsorption and the integration of the foreign elements during lead deposition. This assumption is supported by the fact that in the absence of organic additives, elements such as Cl, C and O were still present even after a long sputtering time, thus indicating that these impurities were trapped within the deposit.

4. Conclusions

1. Lead deposits obtained from glycine–HCl were rough and of the dendritic type on all the cathodes used.

2. The addition of some organic compounds and of gelatine lowered the current density, increased the overpotential and improved the quality of the deposits so that they were smooth, dense and compact in shape.

3. Dendrite formation was promoted in the absence of organic additives in the bath, and a marked deviation from the calculated Tafel slope values for unstirred solutions was observed.

4. Impurities such as C, N and O disappeared quickly as a function of sputtering time for deposits prepared in the presence of organic additives, as indicated by Auger electron spectroscopy studies for both lead and copper electrodes, while these peaks were still shown in the

case of the silver electrode even after 4 h of sputtering.

Acknowledgements

The authors are thankful to the National Science and Engineering Research Council of Canada (NSERC) for providing financial support. Auger facilities offered by the GRAPS laboratories, Laval University, are acknowledged, and special thanks is extended to Dr A. Adnot for his scientific and helpful guidance.

References

[1] K. Naito and F. Habashi, Trans. Inst. Min. Metall. (Section C: Mineral Process. Extr. Metall.) **C69** (1984) 39.

[2] D. J. Mackinnon, in 'Hydrometallurgy Research, Development and Plant Practice', (edited by K. Osseo-Asare and J. D. Miller), AIME, New York (1982) p. G59.

[3] O. A. Khan, in 'Electrometallurgy of Chloride Solutions', (edited by V. V. Stender), translation by Consultants Bureau, New York (1965) p. 127.

[4] A. V. Pomosov, A. I. Levin and E. E. Krymakova, *ibid.*, p. 131.

[5] M. L. Kramer, P. F. Duby and P. D. Parker, in 'Chloride Electrometallurgy' (edited by Peter D. Parker), AIME, New York (1982) p. 77.

[6] F. P. Haver, D. L. Bixby and M. M. Wong, *US Bur. Mines*, R.I. 8276: 11 P: (1978).

[7] E. Ghali and M. Girgis, *Metall. Trans.* **16B** (1985) 489.

[8] M. Girgis, E. Ghali and A. Wieckowski, *Electrochim. Acta* **31** (1986) 681.

[9] M. Girgis and E. Ghali, paper presented at the symposium 'Electrochemistry in Mineral and Metal Processing' at the Spring Meeting of the Electrochemical Society, Cincinnati, Ohio, 6–11 May, 1984.

[10] B. Dandapani and E. Ghali, in 'Chloride Electrometallurgy', (edited by Peter D. Parker), AIME, New York (1982) p. 101.

[11] W. Blum, F. J. Liscomb, Zalia Jencks and W. E. Bailey, *Trans. Amer. Electrochem. Soc.* **27** (1915) 131.

[12] J. A. Harrison, R. P. J. Hill and J. Thompson, *J. Electroanal. Chem.* **44** (1973) 445.

[13] G. Milazzo and S. Caroli, 'Tables of Standard Electrode Potentials', John Wiley and Sons (1978) p. 164.

[14] C. B. Monk, *Trans. Faraday Soc.* **47** (1951) 297.

[15] Robert T. Morrison and Robert N. Boyed, in 'Organic Chemistry', 1st edn, Allyn and Bacon Inc., Boston (1959) p. 861.

[16] L. Kelley, in 'Organic Chemistry', 2nd edn, McGraw-Hill, New York (1964) p. 383.

[17] H. C. Helgson, in 'Complexing and Hydrothermal Ore Deposition', MacMillan, New York (1964).

[18] D. M. Kolb, in 'Advances in Electrochemistry and Electrochemical Engineering', Vol. 11 (edited by Heinz Gerischer and Charges W. Tobias) John Wiley and Sons, New York (1978) p. 125.

[19] E. Schmidt and N. Wüthrich, *J. Electroanal. Chem.* **28** (1970) 349.

[20] S. Stucki, PhD thesis, University of Bern, Switzerland (1973).

[21] J. C. Westall, F. Morel and D. N. Hume, *J. Anal. Chem.* **51** (1979) 1972.

[22] R. S. Nicholson and I. Shain, *J. Anal. Chem.* **36** (1964) 706.

[23] R. G. Barradas, D. A. Rennie and T. J. Vander Noot, *Can. J. Chem.* **63** (1985) 2437.

[24] F. Ogburn, C. Bechtoldt, J. B. Norris and A. Koranyi, *J. Electrochem. Soc.* **112** (1965) 574.

[25] Jung Taek Kim and Jacob Jorné, *ibid.* **127** (1980) 8.

[26] G. Gunawardena, G. Hills, I. Montengro and B. Scharifker, *J. Electroanal. Chem.* **138** (1982) 225.

[27] F. A. Lowenheim, in 'Modern Electroplating', 3rd edn, John Wiley and Sons, New York (1974) p. 27.

[28] 'Handbook of Auger Electron Spectroscopy', JEOL, Tokyo (1982).